On possible small-x effects in the Kaluza-Klein graviton and radion production at high energies

A.V. Lipatov[1,2], M.A. Malyshev[1]

December 13, 2016

[1] *Skobeltsyn Institute of Nuclear Physics, Lomonosov Moscow State University, Moscow 119991, Russia*
[2] *Joint Institute for Nuclear Research, Dubna 141980, Moscow Region, Russia*

Abstract

We study the single graviton production at the CERN LHC using the k_T-factorization approach of QCD. We consider the Arkani-Hamed-Dimopoulos-Dvali scenario and Randall-Sundrum model with one warped extra-dimension and derive the production amplitudes for spin-2 (Kaluza-Klein excitation of the graviton) and spin-0 (radion) states, including subsequent graviton decay into the dilepton or diphoton pairs. We use the transverse momentum dependent (unintegrated) parton densities in a proton obtained from Ciafaloni-Catani-Fiorani-Marchesini (CCFM) evolution equation, which resums the leading logarithmic small-x corrections to the production cross sections. We demonstrate that the small-x effects can manifest themselves in the different angular distributions of graviton decay products and give some examples of how these distributions can look like at the LHC energies.

PACS number(s): 11.10.Kk, 12.38.-t, 12.38.Bx, 13.85.Qk

The scenarios with extra dimensions are ones of the many theoretical schemes which predict new interactions beyond the Standard Model (SM). A generic feature of these scenarios is the presence of Kaluza-Klein (KK) excitations of the graviton, which can be first signature of such physics [1]. The corresponding effects can appear at the TeV energy scale, so that search for extra dimensions is one of the goals of the LHC experiments. Moreover, these scenarios, depending on the geometry of the extra dimensions, can predict relations between the fundamental Planck scale, where gravity becomes strongly coupled, and the weak scale, shedding new light on the hierarchy problem [2–7].

There have been proposed several models with extra dimensions, which can be splitted into two main classes according to the geometry of the background space-time manifold. First of them is the Arkani-Hamed-Dimopoulos-Dvali (ADD) model [2] and its variants, which postulates the existence of $n \geq 2$ large (with common size $R \gg 1/M_p$, where $M_p \sim 10^{19}$ GeV is the 4-dimensional Planck scale) extra dimensions. This model assumes that all the SM particles are localized in the usual spacetime, which is called "brane", while the gravity is allowed to propagate in the additional n-dimensional space compactified on the n-dimensional torus. Then the 4-dimensional Planck scale is a derived scale related to the fundamental Planck scale $M_s \sim 1$ TeV by

$$M_p^2 = M_s^{n+2}(2\pi R)^n, \tag{1}$$

thus solving the hierarchy problem. A solution of the linearized Einstein equation in $4+n$ dimensions results in the appearance of a tower of KK modes, which are separated in mass by $\mathcal{O}(1/R)$ terms. After KK reduction one has massive spin-2 KK gravitons $h^k_{\mu\nu}$ which interact with the SM fields via the SM energy-momentum tensor $T^{\mu\nu}$:

$$\mathcal{L} = -\frac{\kappa}{2}\sum_k T^{\mu\nu}(x)h^k_{\mu\nu}(x), \tag{2}$$

where $\kappa = \sqrt{16\pi}/M_p$ and the summation runs over all KK modes.

The second scenario is the 5-dimensional Randall-Sundrum (RS) model [3] and its variants, which implies a warped metric and the size of the extra dimensions should not be too large compared to the Planck length. This model is based on the solution of Einstein equation for gravity interacting with two branes ("IR" or "SM" brane, where our world is located at high-energy, or "UV" brane) in 5-dimensional space-time, and the 4-dimensional metric is the function of the coordinate of the 5th dimension. It is possible to explain the weakness of the gravitational interaction in comparison with the electroweak one (hierarchy problem) by the existence of warp factor in the metric. There also exist KK towers of massive spin-2 gravitons which interact with the SM fields via the effective Lagrangian [8, 9]:

$$\mathcal{L} = -\frac{1}{M_p^*}T^{\mu\nu}(x)h^0_{\mu\nu}(x) - \frac{1}{\Lambda_\pi}\sum_k T^{\mu\nu}(x)h^k_{\mu\nu}(x), \tag{3}$$

where Λ_π is at the electroweak scale. The coupling of the massless graviton $h^0_{\mu\nu}$ is suppressed by the 4-dimensional reduced Planck scale $M_p^* = M_p/\sqrt{8\pi}$. The mass of the lowest graviton KK mode m_1 and Λ_π can be considered as free parameters which completely determine the graviton sector of RS model, and it is expected that $\Lambda_\pi < 10$ TeV [9, 10]. The quantity

$c_0^* = m_1/x_1\Lambda_\pi$, or rather $c_0 = c_0^*\sqrt{8\pi}$, is also often used as a free parameter. The masses of the kth graviton KK excitation modes are given by

$$m_k = m_1 \frac{x_k}{x_1}, \tag{4}$$

where the x_k are the kth roots of the first order Bessel function. So, the spectrum of KK modes is quite different from one in the ADD scenario.

In the RS model, it is expected that the lightest massive KK graviton can have a mass m_1 of order of several hundred GeV (or even more). Therefore, it can be produced at the LHC and future colliders with relatively high rates. Moreover, its coupling to the SM fields is larger than the one in the ADD model, so that it can decay into observable SM particles and therefore can be detected in collider experiments. The possibility to observe the graviton signal with mass up to several TeV (using the l^+l^-, $\gamma\gamma$, ZZ, W^+W^- and other graviton decay modes) in the proton-proton collisions at the LHC was investigated [11]. The next-to-leading order (NLO) QCD corrections to the virtual graviton production (in the ADD and RS scenarios) were calculated [10,12–14] and Collins-Soper-Sterman resummation formalism was applied [12] to take into account the soft gluon effects in the transverse momentum distributions.

Besides the KK excitation, another common characteristic feature of SM extensions involving extra dimensions is the presence of a massive scalar field (so called the radion field), which has the same quantum numbers as the neutral Higgs field [15–18]. The appearance of the radion field is connected with the spin-0 metric fluctuations due to extra space dimension. Various aspects of the decay and production properties of the radion were investigated [19–27] and it was argued [17, 28] that the radion can be significantly lighter than all the other KK excitations. The interaction vertices of the radion with the SM fields are similar to those of the Higgs boson except for the anomaly enhanced interactions with gluons and photons, that results in the leading role of gluon-gluon fusion production mechanism and corresponding relative enhancement in gluon and photon decay modes.

In the present note we apply the k_T-factorization approach [29, 30] to calculate the total and differential cross sections of KK graviton production (including its subsequent decay into the lepton or photon pair) and radion production at the LHC conditions. This approach is based on the famous Balitsky-Fadin-Kuraev-Lipatov (BFKL) [31] or Ciafaloni-Catani-Fiorani-Marchesini (CCFM) [32] evolution equations and provides solid theoretical grounds for the effects of initial state parton radiation and intrinsic parton transverse momentum. We see certain advantages in the fact that, even with the leading-order (LO) partonic amplitudes, one can include a large piece of higher-order corrections (namely, part of NLO + NNLO + ... terms containing leading $\log 1/x$ enhancement of cross sections due to real initial state parton emissions) taking them into account in the form of transverse momentum dependent (TMD) parton densities in a proton[1]. The latter additionally absorb the effects of soft gluon resummation, which regularises the infrared divergences and makes the k_T-factorization predictions to be applicable even at low transverse momenta [34]. The k_T-factorization approach was applied to number of hard QCD processes at high energies (see, for example, [35–37] and references therein). We perform the calculations for both the ADD and RS scenarios and put a special attention to the angular distributions of KK graviton

[1] A detailed description of the k_T-factorization approach can be found, for example, in reviews [33].

decay leptons or photons since the effects of the initial gluon off-shelness are expected to be observed there.

Let us start from a short review of calculation steps. First we consider the subprocesses where dilepton or diphoton pairs are produced from off-shell gluon-gluon fusion or quark-antiquark annihilation via the virtual KK graviton exchange:

$$\begin{array}{cc} g^*(k_1)+g^*(k_2)\to G^*\to l^+(p_1)+l^-(p_2), & q(k_1)+\bar{q}(k_2)\to G^*\to l^+(p_1)+l^-(p_2), \\ g^*(k_1)+g^*(k_2)\to G^*\to \gamma(p_1)+\gamma(p_2), & q(k_1)+\bar{q}(k_2)\to G^*\to \gamma(p_1)+\gamma(p_2), \end{array} \tag{5}$$

where the four-momenta of all particles are indicated in parentheses. Below we describe the evaluation of the off-shell (transverse momentum dependent) production amplitudes, which are one of the main ingredients of the k_T-factorization approach used. In the center-of-mass frame of colliding protons, having four-momenta l_1 and l_2, we define

$$k_1 = x_1 l_1 + k_{1T}, \quad k_2 = x_2 l_2 + k_{2T}, \tag{6}$$

where x_1 and x_2 are the longitudinal momentum fractions of the protons carried by the interacting off-shell partons having transverse four-momenta k_{1T} and k_{2T} (note that $k_{1T}^2 = -\mathbf{k}_{1T}^2 \neq 0$, $k_{2T}^2 = -\mathbf{k}_{2T}^2 \neq 0$). The relevant Feynman rules were obtained earlier [38], from which we can get the LO amplitudes of the subprocesses (5) as follows:

$$\begin{aligned} \mathcal{M}(g^*g^*\to G^*\to l^+l^-) = \epsilon_{1a}^{\alpha}(k_1)\epsilon_{2b}^{\beta}(k_2)V_{\mu\nu\alpha\beta}^{ab}(k_1,k_2)\Delta_{\nu\mu'\nu'}(k_1+k_2)\times \\ \times\bar{u}_{r_1}(p_1)\Gamma^{\mu'\nu'}(p_1,p_2)v_{r_2}(p_2), \end{aligned} \tag{7}$$

$$\begin{aligned} \mathcal{M}(q\bar{q}\to G^*\to l^+l^-) = \bar{v}_{s_1}(k_2)\Gamma^{\mu\nu}(k_1,k_2)u_{s_2}(k_1)\Delta_{\mu\nu\mu'\nu'}(k_1+k_2)\times \\ \times\bar{u}_{r_1}(p_1)\Gamma^{\mu'\nu'}(p_1,p_2)v_{r_2}(p_2), \end{aligned} \tag{8}$$

$$\begin{aligned} \mathcal{M}(g^*g^*\to G^*\to \gamma\gamma) = \epsilon_{1a}^{\alpha}(k_1)\epsilon_{2b}^{\beta}(k_2)V_{\mu\nu\alpha\beta}^{ab}(k_1,k_2)\Delta_{\mu\nu\mu'\nu'}(k_1+k_2)\times \\ \times V^{\mu'\nu'\alpha'\beta'}(p_1,p_2)e_{1\alpha'}(p_1)e_{2\beta'}(p_2), \end{aligned} \tag{9}$$

$$\begin{aligned} \mathcal{M}(q\bar{q}\to G^*\to \gamma\gamma) = \bar{v}_{s_1}(k_2)\Gamma^{\mu\nu}(k_1,k_2)u_{s_2}(k_1)\Delta_{\mu\nu\mu'\nu'}(k_1+k_2)\times \\ \times V^{\mu'\nu'\alpha'\beta'}(p_1,p_2)e_{1\alpha'}(p_1)e_{2\beta'}(p_2), \end{aligned} \tag{10}$$

where a and b are the eight-fold color indices, $\epsilon_{\mu}^{a}(k)$ and $e_{\mu}(p)$ are the polarization vectors of initial off-shell gluons and produced photons, respectively. In the RS model, the interaction vertices of gluons $V_{\mu\nu\alpha\beta}^{ab}(k_1,k_2)$ and fermions $\Gamma_{\mu\nu}(k_1,k_2)$ with the graviton can be written as

$$V_{\mu\nu\alpha\beta}^{ab} = -i\frac{1}{\Lambda_\pi}\delta^{ab}\left[(k_1\cdot k_2)C_{\mu\nu\alpha\beta} + D_{\mu\nu\alpha\beta}(k_1,k_2) + E_{\mu\nu\alpha\beta}(k_1,k_2)\right], \tag{11}$$

$$\Gamma_{\mu\nu}(k_1,k_2) = -i\frac{1}{4\Lambda_\pi}[\gamma_\mu(k_1-k_2)_\nu + \gamma_\nu(k_1-k_2)_\mu - 2\eta_{\mu\nu}(\hat{k}_1-\hat{k}_2-2m_f)], \tag{12}$$

where m_f is the fermion mass and $\eta_{\mu\nu}$ is the Minkowski metrics tensor. The tensors appear in (11) are defined as [38]

$$C_{\mu\nu\alpha\beta} = \eta_{\mu\alpha}\eta_{\nu\beta} + \eta_{\mu\beta}\eta_{\nu\alpha} - \eta_{\mu\nu}\eta_{\alpha\beta}, \tag{13}$$

$$\begin{aligned} D_{\mu\nu\alpha\beta}(k_1,k_2) = \eta_{\mu\nu}k_{1\beta}k_{2\alpha} - [\eta_{\mu\beta}k_{1\nu}k_{2\alpha} + \eta_{\mu\alpha}k_{1\beta}k_{2\nu} - \\ -\eta_{\alpha\beta}k_{1\mu}k_{2\nu} + (\mu\longleftrightarrow\nu)], \end{aligned} \tag{14}$$

$$E_{\mu\nu\alpha\beta}(k_1,k_2)=\eta_{\mu\nu}(k_{1\alpha}k_{1\beta}+k_{2\alpha}k_{2\beta}+k_{1\alpha}k_{2\beta})- \\ -[\eta_{\nu\beta}k_{1\mu}k_{1\alpha}+\eta_{\nu\alpha}k_{2\mu}k_{2\beta}+(\mu\longleftrightarrow\nu)], \tag{15}$$

and for graviton propagator one has:

$$\Delta_{\mu\nu\alpha\beta}(p)=\frac{(i/2)B_{\mu\nu\alpha\beta}(p)}{p^2-m^2+i\Gamma m}, \tag{16}$$

where m is the graviton mass, Γ is its full decay width and polarization sum $B_{\mu\nu\alpha\beta}(p)$ takes the following form:

$$B_{\mu\nu\alpha\beta}(p)=\eta_{\mu\alpha}\eta_{\nu\beta}+\eta_{\mu\beta}\eta_{\nu\alpha}-\frac{2}{3}\eta_{\mu\nu}\eta_{\alpha\beta}+... \tag{17}$$

The dots represent terms proportional to the graviton momentum p which give a vanishing contribution due to the gauge invariance. Below we neglect the virtualities of the initial quarks in the production amplitudes (8) and (10) compared to the large scale (but not in the kinematics), so that their spin density matrix is taken in the usual form:

$$\sum_{r,s}u_r(p)\bar{u}_s(p)=\hat{p}+m_q, \tag{18}$$

where m_q is the quark mass. According to the k_T-factorization prescription [29, 30], the summation over the polarizations of incoming off-shell gluons is carried with

$$\sum\epsilon^{\mu}(k)\epsilon^{*\nu}(k)=\frac{\mathbf{k}_T^{\mu}\mathbf{k}_T^{\nu}}{\mathbf{k}_T^2}, \tag{19}$$

thus avoiding diagrams involving ghosts. In the limit of collinear QCD factorization, when $\mathbf{k}_T^2\to 0$, this expression converges to the ordinary one after averaging on the azimuthal angle.

The partial decay widths of the KK graviton to SM particles via the Lagrangian (3) are known [38]. So, the partial decay width of the KK graviton to massless gauge bosons $\Gamma_{V_0V_0}$, massive gauge bosons Γ_{VV}, fermions Γ_{ff} and the Higgs boson Γ_{HH} are

$$\Gamma_{V_0V_0}=\frac{Cm^3}{80\pi\Lambda_{\pi}^2}, \tag{20}$$

$$\Gamma_{VV}=\delta\frac{m^3}{40\pi\Lambda_{\pi}^2}\left(1-\frac{4m_V^2}{m^2}\right)^{1/2}\left(\frac{13}{12}+\frac{14m_V^2}{39m^2}+\frac{4m_V^4}{13m^4}\right), \tag{21}$$

$$\Gamma_{ff}=\delta\frac{Cm^3}{160\pi\Lambda_{\pi}^2}\left(1-\frac{4m_f^2}{m^2}\right)^{3/2}\left(1+\frac{8m_f^2}{3m^2}\right), \tag{22}$$

$$\Gamma_{HH}=\frac{m^3}{480\pi\Lambda_{\pi}^2}\left(1-\frac{4m_H^2}{m^2}\right)^{5/2}, \tag{23}$$

where m_V, m_f and m_H are the gauge bosons, fermions and Higgs boson masses, C is the color factor ($C=N_c^2-1$ for gluons, $C=N_c$ for quarks and $C=1$ for colorless particles, where N_c is the number of colors), $\delta=1/2$ for self-conjugate particles and $\delta=1$ for other particles.

To extend the formulas above to the ADD model, one has to replace $1/\Lambda_\pi \to \kappa/2$ and perform the summation over high multiplicity of KK modes lying below the UV cut-off scale (given by M_s). This summation compensates the suppression of each KK mode coupling to the SM particles by Planck mass and gives rise to a substantial effective coupling strength. Following [38, 39], we have to replace the graviton propagator by the effective one:

$$\mathcal{P}_{\text{eff}} = \sum_k \frac{i}{p^2 - m_k^2 + i\Gamma_k m_k}, \tag{24}$$

where k sums over all KK towers below M_s scale. As it was already mentioned above, in the ADD model the mass separation between two adjacent KK modes is a $\mathcal{O}(1/R)$, so that KK modes become quasicontinuous and the summation in (24) can be done by defining KK state density [38, 39]. For n number of extra dimensions, the $\mathcal{P}_{\text{eff}}$ is given by

$$\mathcal{P}_{\text{eff}} = \frac{16\pi \hat{s}^{n/2-1}}{\kappa^2 \Gamma(n/2) M_s^{n+2}} \left[\pi + 2iI\left(\frac{M_s}{\sqrt{\hat{s}}}\right)\right], \tag{25}$$

where $\hat{s} = p^2$ is the invariant mass of the produced dilepton or diphoton pair, and the function $I(\tau)$ reads

$$I(\tau) = \begin{cases} -\sum\limits_{k=1}^{n/2-1} \dfrac{\tau^{2k}}{2k} - \dfrac{1}{2}\ln(\tau^2 - 1), & n = \text{even} \\ -\sum\limits_{k=1}^{(n-1)/2} \dfrac{\tau^{2k-1}}{2k-1} + \dfrac{1}{2}\ln\left(\dfrac{\tau+1}{\tau-1}\right), & n = \text{odd}. \end{cases} \tag{26}$$

The real part of (25) comes from the summation over all resonant contributions below M_s and the imaginary part is the summed contributions coming from all the non-resonant states. Further calculations are straightforward and follow the standard QCD Feynman rules. The evaluation of traces was performed using the algebraic manipulation system FORM [40]. The obtained analytical expressions are too lengthty to be presented here, but they are available from the authors upon request[2].

The amplitude of radion production in the off-shell gluon-gluon fusion can be easily obtained using the effective vertex [20, 26]:

$$T^{\mu\nu}(k_1, k_2) = i\delta^{ab}\frac{\alpha_s}{2\pi}\frac{1}{\Lambda_r}\left[b_{\text{QCD}} + F\left(\frac{4m_t^2}{m_r^2}\right)\right](k_2^\mu k_1^\nu - (k_1 \cdot k_2)g^{\mu\nu}), \tag{27}$$

where a and b are the eight-fold color indices, m_t and m_r are the top quark and radion masses, the radion coupling constant Λ_r is supposed to be of order of electroweak scale, $b_{\text{QCD}} = 7$ and F is the known function (see, for example, [20, 26]). The further evaluation is rather straightforward. We only mention that the summation on the initial off-shell gluon polarizations was done using (19).

To calculate the graviton production cross section in the k_T-factorization approach one has to convolute the relevant off-shell partonic cross section and the TMD parton densities

[2]lipatov@theory.sinp.msu.ru

in a proton. Our master formulas for gluon-gluon fusion and quark-antiquark annihilation read:

$$\sigma = \int \frac{|\bar{\mathcal{M}}|^2}{16\pi (x_1 x_2 s)^2} f_g(x_1, \mathbf{k}_{1T}^2, \mu^2) f_g(x_2, \mathbf{k}_{2T}^2, \mu^2) d\mathbf{p}_{1T}^2 d\mathbf{k}_{1T}^2 d\mathbf{k}_{2T}^2 dy_1 dy_2 \frac{d\phi_1}{2\pi} \frac{d\phi_2}{2\pi}, \tag{28}$$

$$\sigma = \sum_q \int \frac{|\bar{\mathcal{M}}|^2}{16\pi (x_1 x_2 s)^2} f_q(x_1, \mathbf{k}_{1T}^2, \mu^2) f_{\bar{q}}(x_2, \mathbf{k}_{2T}^2, \mu^2) d\mathbf{p}_{1T}^2 d\mathbf{k}_{1T}^2 d\mathbf{k}_{2T}^2 dy_1 dy_2 \frac{d\phi_1}{2\pi} \frac{d\phi_2}{2\pi}, \tag{29}$$

where $f_q(x, \mathbf{k}_T^2, \mu^2)$ and $f_g(x, \mathbf{k}_T^2, \mu^2)$ are the TMD quark and gluon densities in a proton, $|\bar{\mathcal{M}}|^2$ is the corresponding production amplitude squared (and averaged over initial state and summed over final states), $\mathbf{p}_{1T}$, y_1 and y_2 are the transverse momentum and rapidities of produced particles and $\sqrt{s}$ is the pp center-of-mass energy. The similar expression can be obtained for the radion production. In the case of two-photon decay of KK state, one has to include an extra factor 1/2 when integrating over full phase space due to identity of the final state photons. If we average (27) and (28) over ϕ_1 and ϕ_2 and take the limit $\mathbf{k}_{1T}^2 \to 0$ and $\mathbf{k}_{2T}^2 \to 0$, then we recover relevant expressions of LO collinear QCD approximation.

Concerning the TMD quark and gluon densities, we use the CCFM-evolved gluon [41] and valence quark distributions [42] as given by the A0 set, which are commonly recognized and widely applied in the phenomenological applications[3]. The CCFM evolution equation is the most suitable tool for our present study because it smoothly interpolates between the small-x BFKL gluon dynamics and conventional DGLAP one. The corresponding input parameters were fitted from the best description of the proton structure function $F_2(x, Q^2)$. The TMD sea quark density is calculated in the approximation, where the sea quarks occur in the last gluon splitting [44] using the TMD gluon-to-quark splitting function [45].

Numerically, the renormalization and factorization scales μ_R and μ_F were set to $\mu_R^2 = \mu_F^2 = \hat{s} + \mathbf{Q}_T^2$, where $\mathbf{Q}_T$ is the transverse momentum of the initial gluon or quark pair. The choice of μ_F^2 is connected with the CCFM evolution [41]. Other essential parameters were taken as follows. Unless mentioned otherwise, we choosed the parameters $c_0 = 0.01$ for the RS model and $n = 3$ for ADD model and performed calculations for different m_1 and M_s values, respectively. Everywhere we used LO formula for the strong coupling constant $\alpha_s(\mu^2)$ with $n_f = 4$ massless quark flavours and $\Lambda_{\rm QCD} = 200$ MeV, so that $\alpha_s(M_Z^2) = 0.1232$. The multidimensional integration was performed by means of a Monte Carlo technique, using the routine VEGAS [46].

We now are in a position to present our numerical results. In Figs. 1 and 2 we plot the total cross-sections of KK graviton production and its subsequent decays into the dilepton and diphoton pair calculated as a functions of center-of-mass energy for several values of parameters m_1 and M_s (in the RS and ADD models, respectively). Here we compare the k_T-factorization predictions and the ones obtained in the collinear QCD factorization (at the LO level). For the conventional parton densities in a proton, we adopted the LO Martin-Stirling-Thorn-Watt (MSTW'2008) set [47]. One can see that at relatively large values of m_1 or M_s (namely, about of 1 TeV) the k_T-factorization predictions are practically coincide with the LO pQCD ones, and the difference between them occurs only at smaller m_1 or

[3]More recently, another set of the CCFM-evolved parton distributions in a proton, JH'2013 one, was presented [43]. However, the relevant TMD gluon density does not reproduce the behaviour of standard gluon distributions at large x. Therefore, we do not use it in our consideration below.

M_s values. It can be easily understood if we consider the scaling variable $z = m_1/\sqrt{s}$ (or $M_s/\sqrt{s}$), which can serve as an estimation of momentum fraction x of particles involving into the hard interaction. At the LHC energies, this variable is about of $z \sim 0.1$ when m_1 or M_s is about of 1 TeV and going down to $z \sim 5 \cdot 10^{-2}$ for lower m_1 or M_s values (about of 500 GeV). The corresponding "small-x" K-factor, which can be defined as a ratio between tbe k_T-factorization and LO QCD predictions, changes from $K \sim 1$ to $K \sim 1.4 - 1.6$ (see Figs. 1 and 2). As it was mentioned above, the k_T-factorization approach (supplemented with the BFKL or CCFM gluon dynamics) effectively include a part of NLO + NNLO + ... terms containing leading $\log 1/x$ enhancement of cross sections, so that this "small-x" K-factor reflects the role of such terms involved into the total NLO pQCD corrections. According to the estimates [10, 12–14], the latter is about factor of $1.7 - 1.8$ at the LHC conditions[4].

In the considered energy range, the main contributions to the total production cross sections come from the gluon-gluon fusion subprocesses. They give of about 94.8%, 91.1% and 87.1% contributions at $m_1 = 500$, 700 and 900 GeV, respectively. The quark-antiquark initiated subprocesses are suppressed due to large gluon flux at the LHC.

As it is known, the effects connected with the non-collinear parton dynamics can manifest themselves in the different angular correlations between the final state particles [33]. First (and rather trivial) example is the distributions in the azimuthal angle difference $\Delta\phi$ between the produced leptons or photons. In the collinear LO pQCD approximation, this distributions must be simply a delta function $\delta(\Delta\phi - \pi)$, since the produced leptons or photons are back-to-back in the transverse momentum plane. Taking into account the non-vanishing parton transverse momentum leads to violation of this back-to-back kinematics in the k_T-factorization approach even at LO, while in the collinear QCD factorization such violation occurs at NLO level only. The same can be noted for the transverse momentum distributions of produced dilepton or diphoton pairs because the latter is determined by the transverse momenta of incoming partons. These effects are illustrated it in Fig. 3, where we show the p_T^{ll} and $\Delta\phi^{ll}$ distributions calculated in the RS scenario at $c_0 = 0.01$ and $\sqrt{s} = 14$ TeV. As one can see, the k_T-factorization predictions are finite at any p_T^{ll} and $\Delta\phi^{ll}$ values. In the collinear QCD factorization, to make the predictions at low $p_T^{ll} \ll M$ (where M is the invariant mass of dilepton pair) one should use a special soft gluon resummation technique since perturbative QCD calculations at fixed order diverge at small dilepton transverse momenta with terms proportional to $\ln M/p_T^{ll}$ appearing due to soft and collinear gluon emission. However, as it was shown [34], the soft gluon resummation formulas are the result of the approximate treatment of the solution of CCFM evolution equation, implemented in our calculations.

Another example is the distributions in the scattering angle θ^* of KK decay leptons or photons in the KK graviton center-of-mass frame. At LO, the on-shell gluon-gluon fusion processes, which dominate at the LHC energies, behave as $1-\cos^4\theta^*$ and $1+6\cos^2\theta^*+\cos^4\theta^*$ for dilepton and diphoton decay modes, respectively (see, for example, [38, 39]). In the k_T-factorization approach, taking into account the initial gluon off-shellness can result to the deviations from these simple forms, as it is demonstrated in Figs. 4 and 5. For the dilepton KK decay mode, we find that the "small-x" K-factor is more or less flat at $|\cos\theta^*| \leq 0.8 - 0.9$, so that the difference in shape between the k_T-factorization and collinear LO

[4]At very high energies, or, alternatively, in the small-x region, the $\log 1/x$-enhanced terms, corresponding to the real initial-state parton emissions, give the main contribution to the production cross section.

pQCD predictions occurs at $|\cos\theta^*| \geq 0.9$ and becomes more clearly pronounced when the z variable decreases. In the diphoton decay mode, this effect occurs if $|\cos\theta^*|$ is close to zero. In fact, the reason of such shape differences is the presence of additional contributions from the longitudinal polarizations of initial off-shell gluons, which are absent in the collinear QCD calculations. To investigate the influence of off-shell gluon longitudinal polarization in more detail, we repeated these calculations performing the summation over the gluons polarizations explicitly, choosing appropriate expressions for gluon polarization four-vectors. Our results are shown in Fig. 6, where the contributions from different polarizations are displayed separately. As an illustration, we consider here the gluon-gluon fusion only for both dilepton and diphoton decay modes and set $M_s = 500$ GeV (in the ADD model with $n = 3$) to enlarge the visible effect. One can see that the contributions from pure transverse gluon polarizations generally follow the collinear QCD predictions, whereas the contributions from the longitudinal off-shell gluon polarization have different behaviour in $\cos\theta^*$, that leads to the observed deviations from the LO pQCD results. The latter, of course, is embodied in the different polarization of produced particles and, in principle, can be observed experimentally. The same effect was pointed out in the heavy quarkonia production at high energies (see, for example, [48]). As it was demonstrated, the fraction of longitudinally polarized quarkonia increases in the k_T-factorization approach in comparison with the collinear QCD predictions, which is a direct consequence of the enhancement of the longitudinal component in the polarization vectors of initial off-shell gluons. As one can see from Figs. 4 and 5, at the large values of scaling variable z, where the small-x region is not probed, the pointed effect becomes negligible.

Now we turn to the radion production. Our predictions are shown in Fig. 7, where we plot the total cross-sections of radion production calculated as functions of center-of-mass energy and transverse momentum distributions calculated for several values of radion mass. According to estimates [26], the latter can either be of about 125 GeV, or be close to the TeV range, depending on the radion coupling constant. Numerically, we set $m_r = 125$, 500 or 900 GeV with $\Lambda_r = 3$ TeV [26]. As one can see, our predictions follow the same trend as previous ones for graviton production: at relatively large radion mass, $m_r \sim 1$ TeV, there is practically no difference between the k_T-factorization and LO pQCD calculations. The difference occurs at smaller values of radion mass, where essentially small-x region is probed. The predicted transverse momentum distributions, shown in Fig. 7, are finite and determined by the TMD gluon densities in a proton due to $2 \to 1$ subprocess kinematics.

Finally, we would like to note that recent experimental searches performed by the CMS [49, 50] and ATLAS [51, 52] Collaborations put the lower bound on scale M_s quite high: $M_s > 2 - 3$ TeV, thus eliminating the visible small-x effects in the ADD model (which appear at lowest M_s values, as we can see in Figs. 1 and 2). However, even with such large M_s scale, these effects can appear in future collider experiments, like CERN Future Circular Collider (FCC), where total energy of about $\sqrt{s} = 100$ TeV is expected to be reached. Additionally, the recent observation [53, 54] of a 750 GeV resonance in diphoton spectrum at the LHC caused a number of interpretations as a RS graviton (see, for example, [55–58] and references therein). This observation was not confirmed later.

To conclude, we applied the k_T-factorization approach to investigate the Kaluza-Klein graviton production (including its subsequent decay into dilepton and/or diphoton pair) and radion production at the LHC. We considered the Arkani-Hamed-Dimopoulos-Dvali

and Randall-Sundrum scenarios and derived the corresponding amplitudes for spin-2 KK state production and spin-0 radion production in the off-shell gluon-gluon fusion. In the case of subleading quark-induced subprocesses, we neglected the initial quarks transverse momenta in the production amplitudes, but keep the exact off-shell kinematics. We used the transverse momentum dependent quark and gluon densities in a proton obtained from the CCFM evolution equation, which resums the leading logarithmic small-x corrections to the production cross section. It is important that the CCFM equation covers both small-x and large-x regions. We found that the small-x effects (which impact on the overal normalization of calculated cross-sections or polarization of final states) in the KK graviton production at the LHC appear if the lightest graviton mass is of order of 700 GeV or below (in the RS model). The similar conclusion was done for the radion production. In the ADD scenario, the small-x effects appear at $M_s \leq 750$ GeV. We gave some examples of how these effects, connected with the off-shell parton kinematics or additional longitudinal polarization of initial off-shell gluons, can manifest themselves in the different angular distributions of produced particles.

Acknowledgements. We thank E.E. Boos, M.N. Smolyakov, V.E. Bunichev, S.P. Baranov, H. Jung and F. Hautmann for very useful discussions and important remarks. This work was supported in by grant 14-12-00363 of the Russian Science Foundation.

References

[1] M.J. Duff, B.E.W. Nilsson, C.N. Pope, Phys. Rep. **130**, 1 (1986).

[2] N. Arkani-Hamed, S. Dimopoulos, G.R. Dvali, Phys. Lett. **429**, 263 (1998).

[3] L. Randall, R. Sundrum. Phys. Rev. Lett. **83**, 3370 (1999).

[4] J.D. Lykken, Phys. Rev. D **54**, R3693 (1996).

[5] E. Witten, Nucl. Phys. B **471**, 135 (1996).

[6] P. Horava, E. Witten, Nucl. Phys. B **460**, 506 (1996).

[7] I. Antoniadis, Phys. Lett. B **246**, 377 (1990).

[8] J.L. Hewett, Phys. Rev. Lett. **82**, 4765 (1999).

[9] H. Davoudiasl, J.L. Hewett, T.G. Rizzo, Phys. Rev. Lett. **84**, 2080 (2000).

[10] P. Mathews, V. Ravindran, K. Sridhar, JHEP **0510**, 031 (2005).

[11] E.E. Boos, V.E. Bunichev, M.N. Smolyakov, I.P. Volobuev, Phys. Rev. D **79**, 104013 (2009).

[12] Q. Li, C.S. Li, L.L. Yang, Phys. Rev. D **74**, 056002 (2006).

[13] M.C. Kumar, P. Mathews, V. Ravindran, A. Tripathi, Nucl. Phys. B **818**, 28 (2009).

[14] J. Gao, C.S. Li, B.H. Li, C.P. Yuan, H.X. Zhu, Phys. Rev. D **82**, 014020 (2010).

[15] W.D. Goldberger, M.B. Wise, Phys. Rev. Lett. **83**, 4922 (1999).

[16] O. DeWolfe, D.Z. Freedman, S.S. Gubser, A. Karch, Phys. Rev. D **62**, 046008 (2000).

[17] E.E. Boos, Y.S. Mikhailov, M.N. Smolyakov, I.P. Volobuev, Nucl. Phys. B **717**, 19 (2005).

[18] E.E. Boos, Y.S. Mikhailov, M.N. Smolyakov, I.P. Volobuev, Mod. Phys. Lett. A **21**, 1431 (2006).

[19] G.F. Giudice, R. Rattazzi, J.D. Wells, Nucl. Phys. B **595**, 250 (2001).

[20] K.-M. Cheung, Phys. Rev. D **63**, 056007 (2001).

[21] M. Chaichian, A. Datta, K. Huitu, Z.-H. Yu, Phys. Lett. B **524**, 161 (2002).

[22] T.G. Rizzo, JHEP **0206**, 056 (2002).

[23] D. Dominici, B. Grzadkowski, J.F. Gunion, M. Toharia, Nucl. Phys. B **671**, 243 (2003).

[24] J.F. Gunion, M. Toharia, J.D. Wells, Phys. Lett. B **585**, 295 (2004).

[25] E.E. Boos, S. Keizerov, E. Rakhmetov, K. Svirina, Phys. Rev. D **90**, 095026 (2014).

[26] E.E. Boos, V.E. Bunichev, M.A. Perfilov, M.N. Smolyakov, I.P. Volobuev, Phys. Rev. D **92**, 095010 (2015).

[27] E.E. Boos, S. Keizerov, E. Rakhmetov, K. Svirina, Phys. Rev. D **94**, 024047 (2016).

[28] C. Csaki, M.L. Graesser, G.D. Kribs, Phys. Rev. D **63**, 065002 (2001).

[29] L.V. Gribov, E.M. Levin, M.G. Ryskin, Phys. Rep. **100**, 1 (1983);
E.M. Levin, M.G. Ryskin, Yu.M. Shabelsky, A.G. Shuvaev, Sov. J. Nucl. Phys. **53**, 657 (1991).

[30] S. Catani, M. Ciafoloni, F. Hautmann, Nucl. Phys. B **366**, 135 (1991);
J.C. Collins, R.K. Ellis, Nucl. Phys. B **360**, 3 (1991).

[31] E.A. Kuraev, L.N. Lipatov, V.S. Fadin, Sov. Phys. JETP **44**, 443 (1976);
E.A. Kuraev, L.N. Lipatov, V.S. Fadin, Sov. Phys. JETP **45**, 199 (1977);
I.I. Balitsky, L.N. Lipatov, Sov. J. Nucl. Phys. **28**, 822 (1978).

[32] M. Ciafaloni, Nucl. Phys. B **296**, 49 (1988);
S. Catani, F. Fiorani, G. Marchesini, Phys. Lett. B **234**, 339 (1990);
S. Catani, F. Fiorani, G. Marchesini, Nucl. Phys. B **336**, 18 (1990);
G. Marchesini, Nucl. Phys. B **445**, 49 (1995).

[33] B. Andersson *et al.* (Small-x Collaboration), Eur. Phys. J. C **25**, 77 (2002);
J. Andersen *et al.* (Small-x Collaboration), Eur. Phys. J. C **35**, 67 (2004);
J. Andersen *et al.* (Small-x Collaboration), Eur. Phys. J. C **48**, 53 (2006).

[34] A. Gawron, J. Kwiecinski, Phys. Rev. D D **70**, 014003 (2004).

[35] A.V. Lipatov, M.A. Malyshev, N.P. Zotov, Phys. Lett. B **735**, 79 (2014).

[36] S.P. Baranov, A.V. Lipatov, N.P. Zotov, Phys. Rev. D **89**, 094025 (2014).

[37] H. Jung, M. Krämer, A.V. Lipatov, N.P. Zotov, Phys. Rev. D **85**, 034035 (2012).

[38] T. Han, J.D. Lykken, R.J. Zhang, Phys. Rev. D **59**, 105006 (1999).

[39] R. Basu, T. Mandal, Adv. High Energy Phys. **2013**, 652714 (2013).

[40] J.A.M. Vermaseren, NIKHEF-00-023 (2000).

[41] H. Jung, arXiv:hep-ph/0411287.

[42] M. Deak, H. Jung, K. Kutak, arXiv:0807.2403 [hep-ph].

[43] F. Hautmann, H. Jung, Nucl. Phys. B **883**, 1 (2014).

[44] F. Hautmann, M. Hentschinski, H. Jung, arXiv:1205.1759 [hep-ph].

[45] S. Catani, F. Hautmann, Nucl. Phys. B **427**, 475 (1994).

[46] G.P. Lepage, J. Comput. Phys. **27**, 192 (1978).

[47] A.D. Martin, W.J. Stirling, R.S. Thorne, G. Watt, Eur. Phys. J. C **63**, 189 (2009).

[48] S.P. Baranov, Phys. Lett. B **428**, 377 (1998).

[49] CMS Collaboration, Phys. Lett. B **711**, 15 (2012).

[50] CMS Collaboration, Phys. Rev. Lett. **108**, 111801 (2012).

[51] ATLAS Collaboration, Phys. Rev. D **87**, 015010 (2013).

[52] ATLAS Collaboration, New J. Phys. **15**, 043007 (2013).

[53] ATLAS Collaboration, JHEP **09**, 001 (2016).

[54] CMS Collaboration, Phys. Rev. Lett. **117**, 051802 (2016).

[55] M.T. Arun, P. Saha, arXiv:1512.06335 [hep-ph].

[56] S.B. Giddings, H. Zhang, Phys. Rev. D **93**, 115002 (2016).

[57] B.M. Dillon, V. Sanz, arXiv:1603.09550 [hep-ph].

[58] B.M. Dillon, C. Han, H.M. Lee, M. Park, arXiv:1606.07171 [hep-ph].

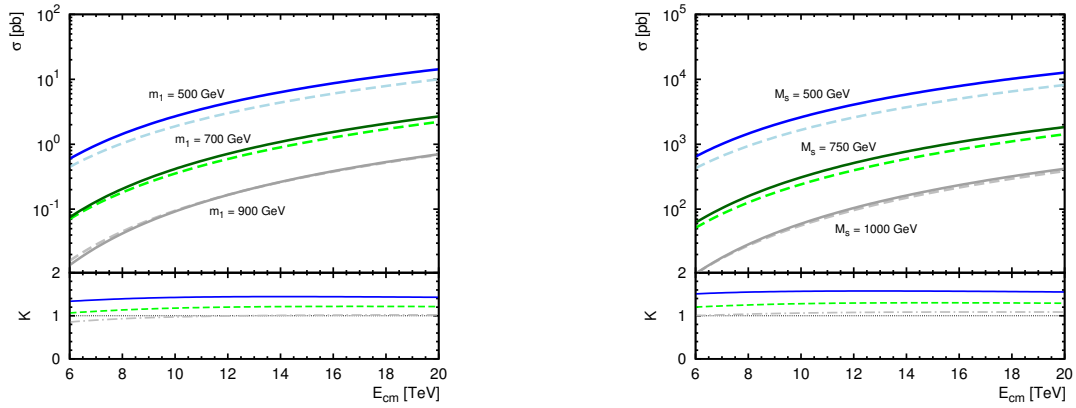

Figure 1: The cross sections of KK graviton production with its subsequent dilepton decay calculated as a function of the total center-of-mass energy in the RS model with $c_0 = 0.01$ (right panel) and ADD model with $n = 3$ (left panel). The solid and dashed curves correspond to the k_T-factorization and LO pQCD predictions, respectively. The ratios of these predictions at $m_1 = 500$, 700 and 900 GeV for RS model and $M_s = 500$, 750 and 1000 GeV for ADD model are shown below by the solid, dashed and dash-dotted curves.

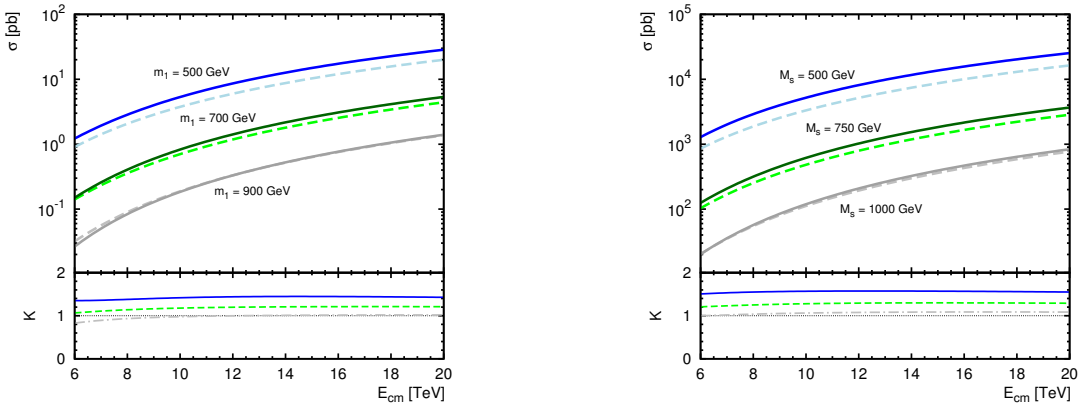

Figure 2: The cross sections of KK graviton production with its subsequent diphoton decay calculated as a function of the total center-of-mass energy in the RS model with $c_0 = 0.01$ (right panel) and ADD model with $n = 3$ (left panel). Notation of all curves is the same as in Fig. 1.

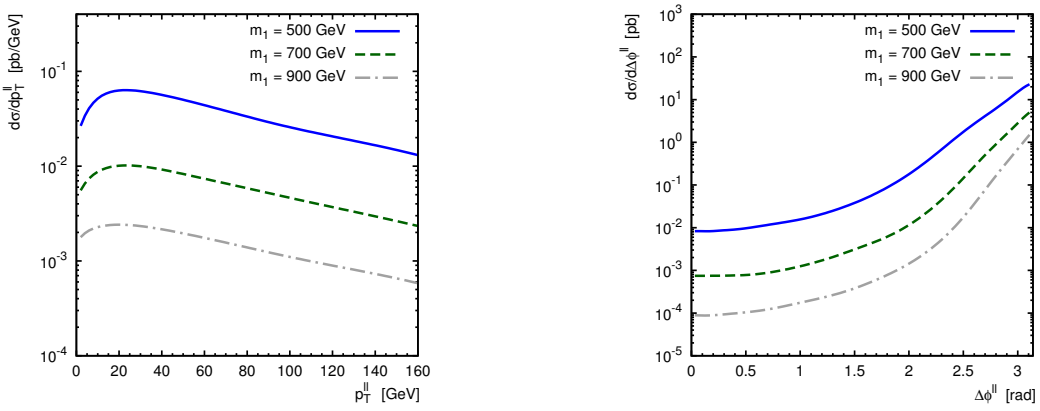

Figure 3: The distributions on the KK decay dilepton transverse momentum p_T^{ll} (right panel) and azimuthal angle difference $\Delta\phi^{ll}$ (left panel) between the four-momenta of these leptons calculated at $\sqrt{s} = 14$ TeV in the RS model with $c_0 = 0.01$. The solid, dashed and dash-dotted curves correspond to $m_1 = 500$, 700 and 900 GeV, respectively.

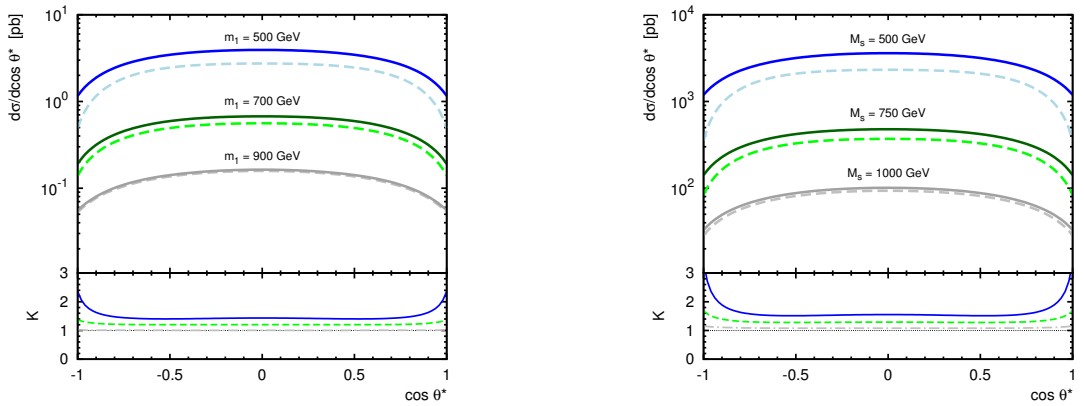

Figure 4: The angular distributions $d\sigma/d\cos\theta^*$ of KK graviton decay lepton pair calculated in the RS model with $c_0 = 0.01$ (right panel) and ADD model with $n = 3$ (left panel) at $\sqrt{s} = 14$ TeV. Notation of all curves is the same as in Fig. 1.

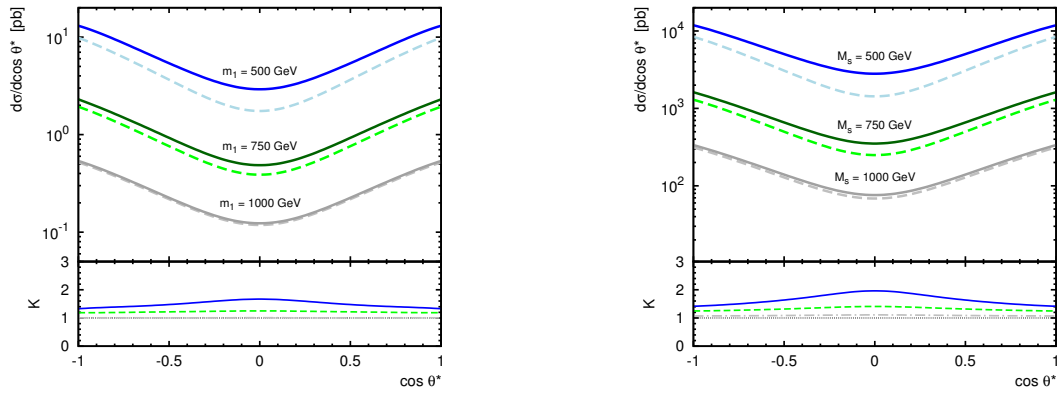

Figure 5: The angular distributions $d\sigma/d\cos\theta^*$ of KK graviton decay photon pair calculated in the RS model with $c_0 = 0.01$ (right panel) and ADD model with $n = 3$ (left panel) at $\sqrt{s} = 14$ TeV. Notation of all curves is the same as in Fig. 1.

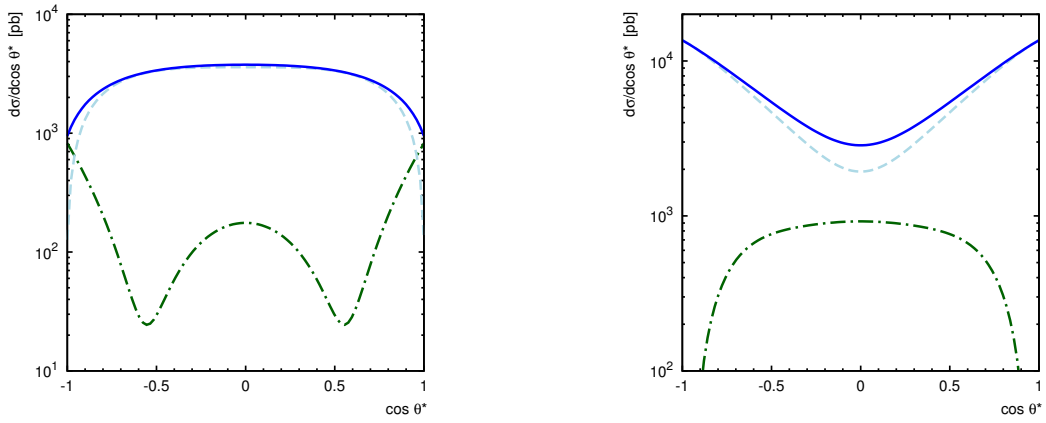

Figure 6: The contributions from transversal and longitudinal off-shell gluon polarizations to the $d\sigma/d\cos\theta^*$ distributions for dilepton (right panel) and diphoton (left panel) KK graviton decay modes calculated in the ADD model with $n = 3$, $M_s = 500$ GeV and $\sqrt{s} = 14$ TeV. The dashed and dash-dotted curves correspond to the transversal and longitudinal components, respectively. The solid curves represent their sum.

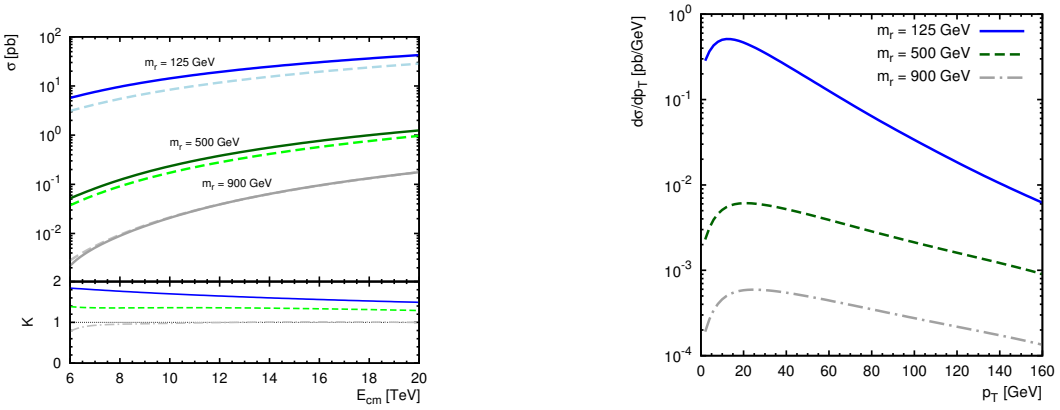

Figure 7: The total cross sections (left panel) and transverse momentum distributions (right panel) of radion production calculated for several values of radion mass m_r at $\Lambda_r = 3$ TeV. Notation of all curves in the left panel is the same as in Fig. 1. The transverse momentum distributions are calculated at $\sqrt{s} = 14$ TeV.